



International Journal for Innovative Engineering and Management Research

A Peer Reviewed Open Access International Journal

www.ijiemr.org

COPY RIGHT



ELSEVIER
SSRN

2019IJIEMR. Personal use of this material is permitted. Permission from IJIEMR must be obtained for all other uses, in any current or future media, including reprinting/republishing this material for advertising or promotional purposes, creating new collective works, for resale or redistribution to servers or lists, or reuse of any copyrighted component of this work in other works. No Reprint should be done to this paper, all copy right is authenticated to Paper Authors

IJIEMR Transactions, online available on 4th Sept 2019. Link

[:http://www.ijiemr.org/downloads.php?vol=Volume-08&issue=ISSUE-09](http://www.ijiemr.org/downloads.php?vol=Volume-08&issue=ISSUE-09)

Title **WIRELESS ELECTRIC VEHICLE CHARGING SYSTEM RECTIFIER LOAD INVESTIGATION**

Volume 08, Issue 09, Pages: 284–301.

Paper Authors

B KASTURI, B SAILAJA, D SANDHYA

Anu Bose Institute of Technology K.S.P Road, New paloncha, Bhadradi Kothagudem, Telangana, India



USE THIS BARCODE TO ACCESS YOUR ONLINE PAPER

To Secure Your Paper As Per **UGC Guidelines** We Are Providing A Electronic Bar Code

WIRELESS ELECTRIC VEHICLE CHARGING SYSTEM RECTIFIER LOAD INVESTIGATION

B KASTURI¹ B SAILAJA² D SANDHYA³

^{1,2,3}UG Students, Dept. of Electrical and Electronics Engineering, Anu Bose Institute of Technology
KSPRoad, NewPaloncha, BhadradriKothagudem, Telangana, India.

bkalyani207@gmail.com¹, sailajasailaja534@gmail.com², sandhya.eee260@gmail.com³

Abstract:-This paper exhibits the investigation of rectifier burden utilized for electric vehicle (EV) remote charging framework, just as its applications on pay system plan and framework load estimation. Initially, a rectifier burden model is built up togetits equal info impedance, which containsboth opposition and inductance parts, and can be autonomously determined through the parameters of the rectifier circuit. At that point, a remuneration system structure strategy is proposed, in light of the rectifier load examination. Besides, an optional side burden estimation technique and an essential side burden estimation strategy are advanced, which embrace just estimated voltages and considerthe impact ofthe rectifier load. At last, an EVremote charging model created, and trial results have demonstrated thatthe rectifier comparable burden canbe accurately determined on states of various framework load protections, rectifier inputs, DC voltages, and shared inductances. Here investigations likewise demonstrate thatrectifierload proportionate inductancewill affect framework exhibitions, andthe proposed strategies of great precision & power inthe instances framework varieties.

Index Terms:-WirelessChargingSystem, RectifierLoad, compensation network design, LoadEstimation

I. INTRODUCTION

ELECTRIC vehicle (EV) remote charging framework (WCS) has the benefits of comfort, space-sparing, and so forth. Along these lines, it has pulled in much consideration. As of late, working standard, activity qualities, framework structure, and control strategy for both stationary and dynamic remote EV charging frameworks have been considered and connected to certain exhibits [1,2]. In uses of EV remote charging, rectifier and yield channel capacitor are expected to change over the high recurrence AC to DC, so as to charge the power battery. Rectifier and the circuit after it are typically proportionate to an unadulterated obstruction burden to plan the

framework or control methodology [3,4]. A customary way is utilizing the coefficient $8/\pi^2$ to make a proportional connection the framework load opposition [5,6]. Be that as it may, strayparameters and non-perfect practices ofthe gadgets will end up clear at the high recurrence extend [7]. Likewise, rectifier input impedance can be influenced by the information inductance and different parameters. Along these lines, it will bring a few deviations, if just considering WCS rectifier input impedance as an unadulterated opposition. As a matter of fact, rectifier input impedance of EV remote charging framework contains both obstruction part and inductance part [7-9]. It

very well may be communicated as a progression of a comparable obstruction and a proportionate inductance [8,9]. In spite of the fact that there has not been a compelling technique to get the identical burden impedance of WCS rectifier, some current inquires about could be useful. In view of the on and off states [10], considering the stray protections and diode forward voltage drop [12]. At that point, the statements of the related voltages and flows have been acquired in the time area, recurrence space, or complex recurrence space [13,14]. It can be utilized for the examination of WCS rectifier identical burden impedance. In addition, non-direct exchanging capacities and circuit reproductions could likewise be received to think about this issue [15]. The non-straight procedure of rectifier burden will carry a few troubles to framework pay system structure. As we probably are aware, pay systems are critical to framework exhibitions [16], and can be intended to accomplish greatest productivity, most extreme power, or conjugate coordinating [17,18]. By and large, an unadulterated opposition is utilized to express rectifier load [19-21]. Be that as it may, the activity methods of WCS rectifier burden will influence the working conditions of pay organize [22]. Along these lines, genuine equal info impedance of WCS rectifier burden ought to be considered, while planning remuneration systems. Burden estimation of WCS has confronted a similar issue. Impacts of the rectifier burden could confuse the conditions utilized for burden estimation [23], and lead to the expanding of computation and control intricacy. Henceforth, an unadulterated opposition burden is around utilized for the vast majority of the heap estimation, discovery, or ideal burden following [24-26]. Another circumstance is that the voltages

and flows are generally estimated for burden estimation, so as to compute the impedances in the essential side [24,27]. Diverse stage delays at the high recurrence run, a few deviations might be brought into the estimation procedure. Likewise, the strength of the estimation technique is significant. It tends to be broke down through parameter deduction, root locus, Nyquist bend, Bode diagram, or legitimately figuring the outcomes on states of parameter varieties [28-30]. In view of the past inquires about, a compelling strategy to quantitatively examine the equal heap of WCS rectifier is advanced in the paper right off the bat. The comparable burden can be autonomously determined through the parameters of the rectifier circuit, and the outcomes are fundamentally not influenced by different WCS parts. Furthermore, a pay system plan technique is proposed considering the comparable impedance of the rectifier load, particularly the proportionate inductance. This technique will further decouple the essential and optional structure, to accomplish four framework execution pointers simultaneously. Thirdly, the impacts of the rectifier non-direct procedure are taken into tally to appraise the framework load obstruction. The proposed essential side burden estimation strategy just receives high recurrence voltages, does not have to gauge flows, and can maintain a strategic distance from the stage defer deviations. Likewise, it doesn't require remote correspondence between the essential and optional sides. This article is sorted out as follows. Area II builds up the rectifier burden model and demonstrates the proportionate info impedance counts. Area III exhibits the remuneration system plan technique. Segment IV proposed the heap estimation techniques dependent on essential and auxiliary side voltage estimations. Segment

V gives the exploratory confirmations and dialogs.

II. RECTIFIERLOAD ANALYSIS AND CALCULATION

Full-connect diode rectifier is the most ordinarily utilized topology in EV remote charging framework. Likewise, double side LCC pay systems can give a few suitable plan degrees of opportunity to accomplish a few framework execution pointers simultaneously. In addition, it very well may be intended to make the framework resounding recurrence autonomous of the heap condition [16,22]. So we talk about the rectifier load based on this sort of topology.

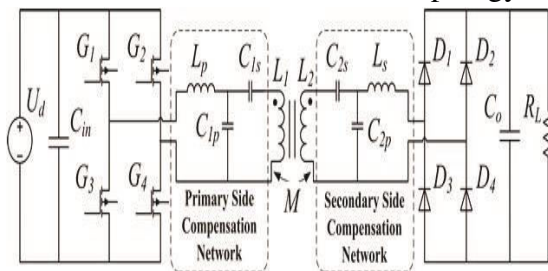


Fig. 1. EV remote charging arrangement of full-connect diode rectifier and double side LCC pay systems.

Fig.1 demonstrates the EV remote charging arrangement of full-connect diode rectifier and double side LCC remuneration systems; where, U_d is DC voltage source; the high frequency inverter is made out of G_1 - G_4 , and the full-bridge rectifier is made out of D_1 - D_4 ; the essential side pay system comprises of L_p , C_{1s} , and C_{1p} ; the auxiliary side pay system comprises of L_s , C_{2s} , and C_{2p} ; L_1 and L_2 are self-inductances of the transmit loop and get curl; M is common inductance between them; C_{in} and C_o are framework information and yield channel capacitors; R_L is framework load resistor. It ought to be seen that the WCS burden is an EV control battery in the reasonable case, which carries on a voltage source arrangement with its parasitic opposition. In any case, the power battery could be equal

to a heap obstruction RL [1,19]; the estimation of this comparable opposition can be determined by the voltage on the power battery separated by the present moving through it. In addition, the full-bridge rectifier, its info inductor, yield channel capacitor, and the heap resistor are as one characterized as the rectifier circuit. Despite the fact that the accompanying investigation is led dependent on the particular framework, it very well may be stretched out to applications on other rectifier and remuneration arrangement topologies.

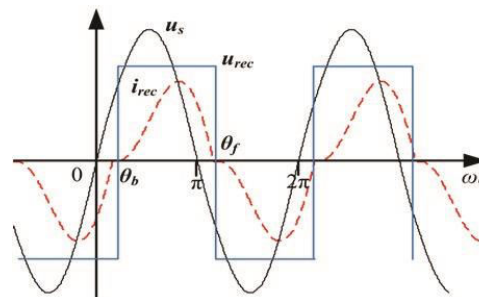


Fig. 2. Schematic waveforms of the source voltage, rectifier input voltage and current.

So as to ascertain rectifier equal info impedance, we right off the bat need to break down the voltages and flows of rectifier circuit, which are appeared in Fig.2; is chosen as the facilitate zero of x-pivot. θ_b and θ_f are begin and end stage points of u_{rec} and i_{rec} . So, $\theta_f = \theta_b + \pi$. Likewise, the rectifier input inductance L_s ought to be enormous enough to keep the rectifier working in the nonstop conduction mode (CCM), so as to maintain a strategic distance from too huge current crests in the diodes. Consequently, just CCM states are appeared in Fig.2, and talked about in this paper. Furthermore, the enduring state waveforms of u_{rec} and i_{rec} are displayed in Fig.2, when just a couple of variances exist on the voltage of the yield capacitor C_o and the voltage drop on R_{Co} is little. In this way, u_{rec} can be roughly portrayed as a square wave. Fig.2

recommends that the waveform of rectifier input current i_{rec} has some bending, due with the impact of the rectifier input inductance. This makes the crucial rush of i_{rec} falls behind the one of u_{rec} . In this way, the rectifier input impedance does incorporate obstruction segment, yet additionally contains a specific inductance part. In addition, Fig.2 demonstrates that the positive and negative half-cycles are symmetric for all the voltage and current waveforms. Henceforth, simply needed to think about the positive half-cycle, and the negative half-cycle can be acquired from the symmetry. Fig.3 demonstrates the proportional drop; where, u_{dio} speaks to the diode forward voltage drop; R_{dio} is diode conduction opposition; R_{L_s} and R_{C_o} are stray protections of L_s and C_o , separately; u_d and i_d are load voltage and current.

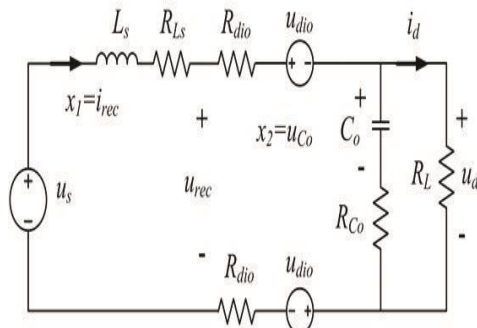


Fig. 3. Proportionate circuit of the rectifier circuit in the positive half cycle.

In light of the proportional circuit, i_{rec} is characterized as state variable x_1 , and the voltage on C_o characterized as state variable x_2 . u_s and u_{dio} are treated as the information factors, and u_d is the yield variables. Along these lines, state space condition of the rectifier circuit is given (1a).

$$\begin{bmatrix} \dot{x}_1 \\ \dot{x}_2 \end{bmatrix} = \mathbf{A} \begin{bmatrix} x_1 \\ x_2 \end{bmatrix} + \mathbf{B} \begin{bmatrix} u_s \\ u_{dio} \end{bmatrix}, \quad y = \mathbf{C} \begin{bmatrix} x_1 \\ x_2 \end{bmatrix}.$$

Where, impedance lattices \mathbf{A} , \mathbf{B} , and \mathbf{C} were given

$$\mathbf{A} = \begin{bmatrix} -\frac{1}{L_s} (R_{L_s} + 2R_{dio} + \frac{R_L R_{C_o}}{R_L + R_{C_o}}) & -\frac{1}{L_s} (1 - \frac{R_{C_o}}{R_L + R_{C_o}}) \\ \frac{R_L}{C_o (R_L + R_{C_o})} & -\frac{1}{C_o (R_L + R_{C_o})} \end{bmatrix}$$

$$\mathbf{B} = \begin{bmatrix} 1/L_s & -2/L_s \\ 0 & 0 \end{bmatrix}, \quad \mathbf{C} = \begin{bmatrix} \frac{R_L R_{C_o}}{R_L + R_{C_o}} & 1 - \frac{R_{C_o}}{R_L + R_{C_o}} \end{bmatrix}.$$

At that point, the information factors and the underlying estimations of the state factors are given by (2), as per the schematic waveforms in Fig.2; where, ω is framework edge recurrence; the diode forward voltage drop is treated as a consistent worth V_{dio} . Since just a couple of vacillations exist on the voltage of C_o and the voltage drop on R_{C_o} is extremely little, persuasions can be overlooked, and the underlying value of x_2 can be around proportionate to a DC voltage variable V_d . Likewise, adequacy of us is characterized as V_s , and it will be influenced by WCS parameters, for example, source voltage, common inductance, and so forth. Be that as it may, the amplitudes of u_{rec} and i_{rec} are relative to V_s . Along these lines, V_s can be treated as a known variable.

$$u_{s+} = V_s \sin(\omega t + \theta_b), \quad u_{dio} = V_{dio}, \quad x_2(0) = [0, V_d]^T.$$

Furthermore, V_d and θ_b should be calculated to solve the state space equation. On the WCS normal working conditions, the value of V_{dio} and the voltage drops on R_{dio} and R_{L_s} are much smaller than the ones of V_s and V_d . So, the voltage on L_s is approximately equivalent to $V_s \sin \theta - V_d$, and the expression of i_{rec} can be given by (3), according to the relationship between the voltage on an inductor and the current flowing through it.

$$i_{rec} = \frac{1}{\omega L_s} \int_{\theta_b}^{\theta} (V_s \sin \theta - V_d) d\theta.$$

As shown in Fig.2, $i_{rec} = 0$, when $\theta = \theta_b + \pi$. So, one relationship between V_d and θ_b can be got and given by (4).

$$V_d = (2V_s \cos \theta_b) / \pi.$$

Additionally, the DC load current I_d can be determined by (5), which is the normal

estimation of i_d in the positive half cycle.

$$I_d = \frac{1}{\pi \omega L_s} \int_{\theta_b}^{\theta_b + \pi} \int_{\theta_b}^{\theta} (V_s \sin \theta - V_d) d\theta$$

$$= (V_s (2 \sin \theta_b + \pi \cos \theta_b) - \pi^2 V_d / 2) / \pi \omega L_s.$$

Because $I_d = V_d / R_L$, another relationship between V_d and θ_b can be got and given by (6).

$$V_d = V_s (2 \sin \theta_b + \pi \cos \theta_b) / (\pi (\omega L_s / R_L + \pi / 2)).$$

In light of the two connections among V_d and θ_b , they can be gotten from (4) and (6). The statement of θ_b is given by (7), and the declaration of V_d can likewise be got by their connections. Condition (7) shows that the stage contrast among us and u_{rec} (or i_{rec}) is chiefly chosen by L_s and R_L , and around autonomous of different WCS parameters. Since scales of u_{rec} and i_{rec} are fundamentally relative to the one of us as referenced above, we can say that different pieces of WCS have little impact on the rectifier circuit & the rectifier burden can be decoupled to dissect its identical information impedance. It is ought to be seen that the rectifier circuit is by all accounts comparable to an unadulterated resistance R_L , as indicated by (7). In any case, this identical relationship is appropriate for (7) when ascertaining the stage edge θ_b , and can't be utilized for some other part in the rectifier load examination.

$$\theta_b = \arctan(\omega L_s / R_L).$$

In the wake of getting V_d and θ_b , full reaction of the rectifier circuit in the positive half cycle can be determined by (8); where, $\Phi(t)$ is the trademark framework of rectifier circuit; the part before the in addition to sign is utilized for settling zero-input reaction, and the other part is utilized for unraveling zero states reaction. Based on (8), time space articulations of u_{rec} and i_{rec} can be acquired, as indicated by the symmetry of their waveforms.

$$x(t) = \Phi(t)x(0) + \int_0^t \Phi(t-\tau) B u(\tau) d\tau$$

$$= e^{A t} \begin{bmatrix} 0 \\ V_d \end{bmatrix} + \int_0^t e^{A \tau} B \begin{bmatrix} V_s \sin(\omega(t-\tau) + \theta_b) \\ V_{dio} \end{bmatrix} d\tau.$$

At last, the principal wave amplitudes and stage points of u_{rec} and i_{rec} can be determined through Fourier change, and characterized as U_{rec_fi} , I_{rec_fi} , ω_{urec_fi} , and ω_{irec_fi} . So, the equivalent input impedance of WCS rectifier load will be given by (9); where, R_e and L_e are arrangement equal opposition and inductance of the rectifier load. Just key wave is considered, on the grounds that the intensity of the sounds is a lot littler than the one of the principal wave. Be that as it may, the symphonious information impedances can likewise be acquired from Fourier change. Additionally, the figuring procedure proposes R_e and L_e will be influenced by the parameters of the rectifier circuit. Subsequently, the strength of this technique towards parameter variety should be considered. In any case, the hypothetical techniques, for example, computing the Subsidiary and root locus can't give a basic and clear approach to break down the power for this situation, since it is identified with some mind boggling or non-straight tasks. Along these lines, this issue will be talked about in Section V, in light of the real parameter ω .

$$R_e = (U_{rec_fi} / I_{rec_fi}) \cos(\varphi_{urec_fi} - \varphi_{irec_fi}),$$

$$L_e = (U_{rec_fi} / I_{rec_fi}) \sin(\varphi_{urec_fi} - \varphi_{irec_fi}) / \omega.$$

To whole up, the above examination proposes that the rectifier load proportional impedance contains both obstruction and inductance parts. Likewise, arrangements of identical obstruction and inductance can be freely determined through parameters of rectifier circuit, and the outcomes are essentially not influenced by different WCS parameters. Along these lines, the rectifier burden can be decoupled with different

pieces of WCS, and make framework structure simpler.

III. COMPENSATION NETWORK DESIGN

Since the rectifier burden has been decoupled with different pieces of WCS, we will propose a remuneration system structure technique, in view of the rectifier load investigation and some current inquires about [16-18]. Additionally, the proposed strategy will further decouple the essential and optional side structure, and make the WCS pay system plan easier. As same as the rectifier load examination, the double side LCC remuneration systems are utilized here. so we will affirm it before the pay system structure. Likewise, the essential side pay inductance L_p is thought to be known, and just the four remuneration capacitors are utilized in the structure technique in this area.

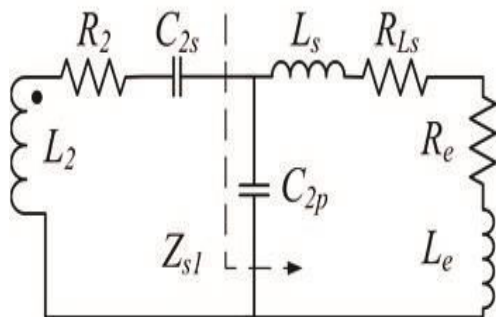


Fig. 4. Equivalent circuit

Right off the bat, the optional side is talked about, and its proportional circuit is appeared in Fig.4; where, the arrangement proportionate opposition R_e and comparable inductance L_e are utilized to express the rectifier load; R_2 is obstruction of the get curl. As appeared in Fig.4, Z_{s1} is characterized as the impedance after the optional side arrangement pay capacitor C_{2s} , given by (10); where,

$R_e' = R_e + R_{L_e}$; $L_e' = L_e + L_{L_e}$; $re(Z_{s1})$ means the real part of Z_{s1} ; $im(Z_{s1})$ is the imaginary part of Z_{s1} .

$$re(Z_{s1}) = \frac{R_e' / (\omega^2 C_{2p}^2)}{R_e'^2 + (\omega L_e' - 1 / (\omega C_{2p}))^2}$$

$$im(Z_{s1}) = - \frac{R_e'^2 / (\omega C_{2p}) + L_e' (\omega L_e' - 1 / (\omega C_{2p})) / C_{2p}}{R_e'^2 + (\omega L_e' - 1 / (\omega C_{2p}))^2}$$

Along these lines, articulation of the productivity η_c can be determined and given by (11); where, η_c is the effectiveness from inverter yield to rectifier load impedance; R_1 is opposition of the transmit curl; $X_{se} = im(Z_{s1}) + \omega L_2 - 1 / (\omega C_{2s})$.

$$\eta_c = \frac{re(Z_{s1}) \omega^2 M^2}{(re(Z_{s1}) + R_2) \omega^2 M^2 + (re(Z_{s1}) + R_2)^2 R_1 + R_1 X_{se}^2}$$

Condition (11) shows that two conditions should be met, for accomplishing most extreme effectiveness. One is $X_{se} = 0$ to limit the denominator of η_c . The other is the heap obstruction of the get loop is equivalent to the ideal burden opposition R_{opt} , as given by (12); where, R_{opt} are obtained from the derivation of η_c , when $X_{se} = 0$.

$$re(Z_{s1}) = R_{opt} = \sqrt{R_2^2 + \omega^2 M^2 R_2 / R_1}$$

On the basis of (10) and (12), the secondary side parallel remuneration capacitor C_{2p} can be determined and given by (13). As per the estimation of C_{2p} and the condition $X_{se} = 0$, the auxiliary arrangement pay capacitor C_{2s} can likewise be tackled. The above investigation recommends that the optional side pay capacitors can be structured autonomously of the essential side ones, and their plan designs for the most part to accomplish greatest framework proficiency.

$$C_{2p} = \frac{\omega L_e' + \sqrt{\omega^2 L_e'^2 - (R_e'^2 + \omega^2 L_e'^2)(1 - R_e' / R_{opt})}}{\omega (R_e'^2 + \omega^2 L_e'^2)}$$

Then, the primary side is studied, and its equivalent circuit is shown in Fig.5; where, u_{inv} is inverter output equivalent voltage source; R_{Lp} is stray resistances of L_p ; R_{es} is the equivalent resistance of the secondary side, when C_{2s} and C_{2p} are well designed, and $R_{es} = \omega^2 M^2 / (R_{opt} + R_2)$.

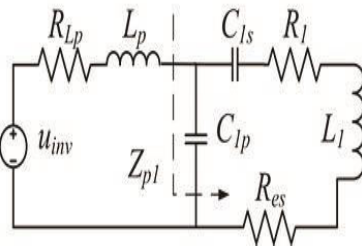


Fig. 5. Equal circuit of the framework essential side, when the auxiliary side is very much structured.

$$re(Z_{p1}) = \frac{(R_{es} + R_1) / (\omega^2 C_{1p}^2)}{(R_{es} + R_1)^2 + X_{pe}^2},$$

$$im(Z_{p1}) = -\frac{(R_{es} + R_1)^2 + X_{pe}(\omega L_1 - 1/(\omega C_{1s}))}{\omega C_{1p}((R_{es} + R_1)^2 + X_{pe}^2)}.$$

As shown in Fig.5, Z_{p1} is defined as the impedance after the primary side compensation inductor L_p , and its expression is given by (14); where, $X_{pe} = \omega L_1 - 1/(\omega C_{1s}) - 1/(\omega C_{1p})$; $re(Z_{p1})$ means the real part of Z_{p1} ; $im(Z_{p1})$ is the imaginary part of Z_{p1} .

Similar with the secondary side design, the primary side also contains two compensation capacitors with two degrees of freedom for design. So, two design targets could be added here. The first one is making the WCS output rated power. The corresponding target equation is given by (15); where, U_{inv} is the RMS value of u_{inv} ; P_{or} is the rated WCS output power; η_r is the rated WCS efficiency.

$$U_{inv}^2 / re(Z_{p1}) = P_{or} / \eta_r.$$

The subsequent structure target is keeping the info impedance of the essential remuneration system containing a specific inductance, so as to understand the delicate exchanging of the inverter. The comparing objective condition is given by (16); where, L_{soft} is the inductance required for inverter delicate exchanging.

$$im(Z_{p1}) / \omega + L_p = L_{soft}.$$

Through at the same time tackling (15) and (16), estimations of the essential side remuneration capacitors C_{1s} and C_{1p} can be acquired, which isn't influenced by the auxiliary side structure process. Additionally, it ought to be seen that occasionally there is no expository answer for these conditions. Numerical arrangement techniques should be utilized on this condition.

At last, the essential and optional side pay systems have been decoupled for structure. Additionally, four remuneration capacitors with four degrees of opportunity are planned by considering four framework execution pointers, including accomplishing most extreme proficiency, ideal burden obstruction, making WCS yield evaluated control, and understanding the delicate exchanging of the inverter. In addition, determined estimations of the planned pay capacitors require tweaking practically speaking to show signs of improvement results.

IV. LOAD ESTIMATION METHODS

The rectifier load examination results can be utilized for framework load estimation, which receiving the high recurrence flag in WCS. The traditional burden estimation techniques are normally founded on the unadulterated obstruction burden, and furthermore need the high recurrence voltage and current simultaneously [24,27]. The voltage and current sensors or tests will have diverse stage delays at the high recurrence extend, incorporating the ones utilized in oscilloscopes and power analyzers. These diverse stage defers will prompt a few deviations of the stage edge between the deliberate voltage and current, and influence the exactness of the

impedance computation, particularly when the stage point is near 90° . So as take care of this issue, we proposes a heap assessment technique dependent on the optional side high recurrence voltages. The particular procedure is as per the following: right off the bat, the are identified, so as to get the positive zero intersection times. At that point, characterize the positive zero intersection time ofthe voltage before rectifier inputinductor as tucs, and the accompanying positive zero intersection time ofthe rectifier input voltage turs. Along these lines, the heap estimation articulation is given by (17), as indicated by the relationship appeared in (7). At long last, since WCS hasbeen worked burden estimation, the estimation of the rectifier inputinductorLs can be estimated, and framework point recurrence ω is likewise. Along these lines, the assessed burden RL_Sesticanbe determined through (17). It proposes optional site burden estimation technique hasconsidered the impact ofthe WCS rectifier load. Likewise, just high recurrence voltages are utilized in this technique; no current is received. Consequently, it can maintain a strategic distance from the deviations presented by various stage delays between estimated voltageandcurrent. Additionally, the proposed strategy just distinguishes the positive zero intersection times. This will carry a few rearrangements to the relating estimations and figurings. Notwithstanding, the deliberate flag still should be transmitted to the essential side by remote correspondence much of the time, utilized for framework improvement or control. So as to maintain a strategic distance from the issues brought by remote correspondence, we further set forward a heap estimation technique dependent on the essential side high recurrence voltages. Characterize the

essential voltage move work between the inverter yield voltage and the voltage after inverter yield inductor as G_p , and the basic voltage move work between the voltage before rectifier input inductor and the rectifier input voltage as G_s . The stage edge of G_s will be θ_b as characterized in Fig.2, which can be embraced for burden estimation dependent on (7). In this way, we have to discover a connection among G_s and G_p , and afterward the deliberate essential side voltages can be utilized to compute θ_b . To accomplish this, some WCS parts can be treated as a two-port system [17,18]. Subsequently, the coupling loops and pay capacitors are proportionate to a two-port system as appeared in Fig.6.

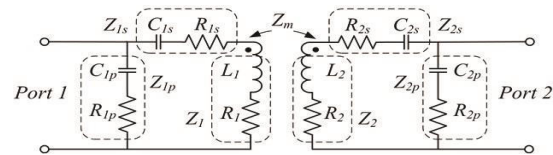


Fig. 6. Schematic of the proportional two-port system and its parameters. As indicated by Fig.6, impedance parameters of the equal two-port system can be determined and given by (18a).

$$Z_{11} = Z_{1p}((Z_1 + Z_{1s})(Z_2 + Z_{2s} + Z_{2p}) - Z_m^2) / \text{den},$$

$$Z_{12} = Z_{21} = Z_{1p}Z_{2p}Z_m / \text{den},$$

$$Z_{22} = Z_{2p}((Z_2 + Z_{2s})(Z_1 + Z_{1s} + Z_{1p}) - Z_m^2) / \text{den}.$$

Where, $Z_m = j\omega M$, and the denominator den is defined by (18b).

$$\text{den} = (Z_1 + Z_{1s} + Z_{1p})(Z_2 + Z_{2s} + Z_{2p}) - Z_m^2.$$

Then, the association between G_s and G_p can be became and given by (19a), based on the impedanceparameters of theequivalenttwoportnetwork.

$$G_s = (n_1 G_p + n_2) / (d_1 G_p + d_2).$$

Where, the coefficients n_1 , n_2 , d_1 , and d_2 are defined by (19b);

Where, $Z_p = R_{Lp} + j\omega L_p$; $Z_s = R_{Ls} + j\omega L_s$.

$$n_1 = Z_{12}Z_{21} - Z_{11}Z_{22}, \quad d_2 = (Z_{11} + Z_p)(Z_{22} + Z_s) - Z_{12}Z_{21},$$

$$n_2 = Z_pZ_{22} + Z_{11}Z_{22} - Z_{12}Z_{21}, \quad d_1 = Z_{12}Z_{21} - Z_{11}(Z_{22} + Z_s).$$

Moreover, the amplitudes and stage points of the chose voltages will be estimated in the essential side, and after that the exchange work G_p can be gotten. Characterize the abundancy of G_p as Amp , and the stage point of G_p as Php . In this way θ_n , which is the stage edge of the numerator of G_s , can be determined, as well as θ_d , which is the stage edge of the denominator of G_s . Their looks are given by (20).

$$\theta_n = \arctan \frac{Amp \cdot amn1 \cdot \sin(Php + phn1) + imn2}{Amp \cdot amn1 \cdot \cos(Php + phn1) + ren2}$$

$$\theta_d = \arctan \frac{Amp \cdot amd1 \cdot \sin(Php + phd1) + imd2}{Amp \cdot amd1 \cdot \cos(Php + phd1) + red2}$$

Where, $amn1$ and $phn1$ are the abundancy and stage edge of $n1$; $amd1$ and $phd1$ are the adequacy and stage edge of $d1$; $ren2$ and $imn2$ are the genuine and nonexistent pieces of $n2$; $red2$ and $imd2$ are the genuine and fanciful pieces of $d2$; they can be determined through (18) and (19), as indicated by the deliberate estimations of the WCS parameters. C_{1s} , C_{1p} , C_{2s} , C_{2p} , etc. Consequently, the strength of the estimation techniques should be examined, when these parameters shift. Be that as it may, comparable with the instance of the rectifier equal burden figuring technique in Section II, the hypothetical strategies can't give a basic and clear approach to break down the vigor. Along these lines, this issue will be additionally examined in Section V, in view of the genuine parameter esteems.

$$R_{L_Pestii} = \omega L_s / \tan(\theta_n - \theta_d)$$

Created from the above optional side burden estimation strategy, the proposed essential side burden estimation technique has additionally considered the impact of the rectifier load. In the mean time, it just embraces high recurrence voltages, and can keep away from the stage defer deviations, as well. The thing that matters is this technique needs to gauge voltage amplitudes. Be that as it may, on the

opposite side, it doesn't require remote correspondence between the essential and auxiliary sides. In this way, it has a few favorable circumstances in EV applications.

V. EXPERIMENTAL VERIFICATION AND ANALYSIS

A. Experiment Layout and System Parameters

An EV remote charging model created to confirm the rectifier load investigation results and the proposed techniques. Its setup appeared in the photo in Fig. 7. A full-connect single-stage inverter with MOSFETs is relegated as the power source. Framework burden is a full-connect diode rectifier with burden resistors. The transmit curl is adjusted rectangular with winding plate sort of fifteen turns of Litz wires. The get loop is square with winding circle kind of twenty turns of Litz wires. The Litz wire utilized for loops is 640 strands with 0.1 mm measurement for each strand. Likewise, ferrites are received as the center material of the curls, and aluminum plates are included outside the ferrites for all the more protecting. The transmit loop size is 58 cm \square 42 cm, and the get curl size is 32 cm \square 32 cm. The vertical separation between the curls is 20 cm.

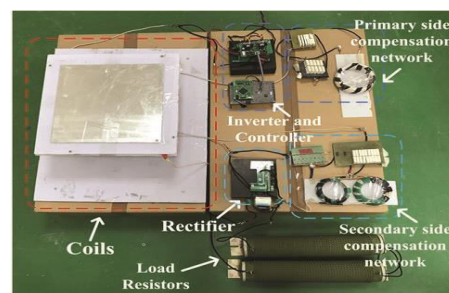


Fig. 7. Photo of the created EV remote charging model.

The model is structured appraised yield control 3.3 kW on the information DC voltage 400 V. Framework activity recurrence is 85 kHz. Burden obstruction RL is 42.9 Ω , which is chosen by an EV control battery with around 325 V - 340 V

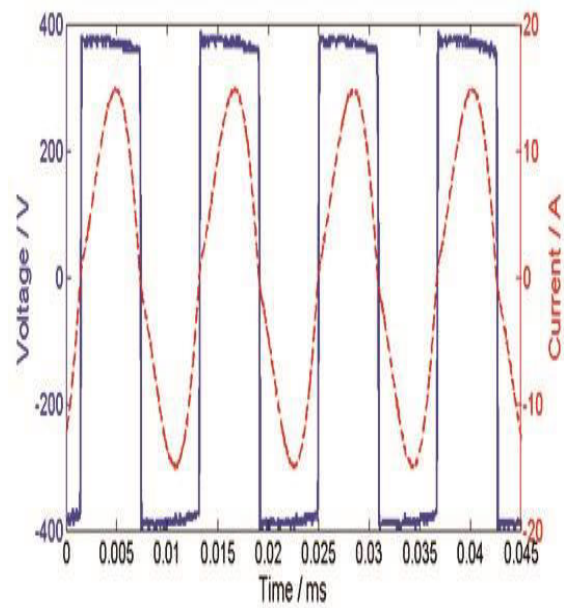
current. Framework impedance parameter esteems are estimated by a LCR meter, and the outcomes are given as pursues. Self-inductances estimations of the transmit loop and get curl are 232.9 uH and 219.7 uH. Common inductance worth is 25.4 uH, when the get loop is lined up with the transmit curl. Pay inductors L_p and L_s are chosen to be 79.9 uH and 83.3 uH. In view of the plan strategy in Section III, the pay capacitors can be gotten as pursues: $C1s=19.7$ nF, $C1p=82.8$ nF, $C2s=23.6$ nF, $C2p=69.6$ nF. The above parameter esteems are characterized as the standard parameter esteems, which can cause the framework to accomplish great exhibitions, for example, appraised yield control, high productivity, inverter delicate exchanging, and so forth. In the accompanying areas, a portion of these parameters will be changed to various qualities for further confirmations and exchanges. The kind of MOSFET is IPW65R037C6. Additionally, the estimations of V_{dio} and R_{dio} will change with the intersection temperature T_j (in degrees Celsius), as appeared in the datasheet of the diode C3D16060D, which is utilized in the created model. In this way, their qualities can be gotten from the deliberate temperature by a warm imager and the accompanying conditions in the datasheet:

$$V_{dio} = 0.93 + ((-9.3 \times 10^{-4}) \times T_j); R_{dio} = 0.058 + ((5.7 \times 10^{-4}) \times T_j).$$

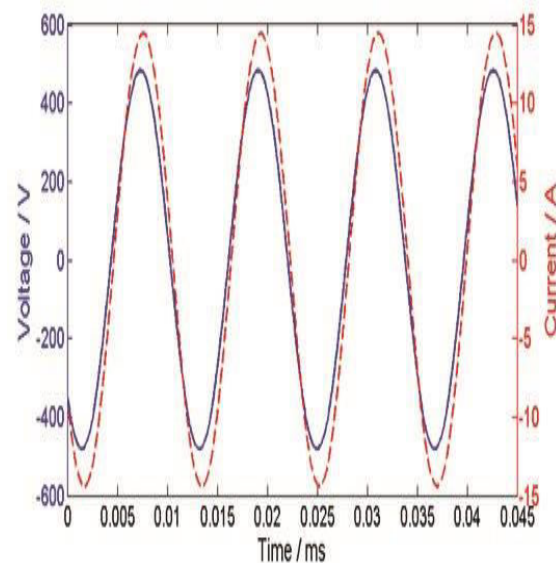
B. Rectifier Equivalent Load Verifications and Analysis

In view of the created EV remote charging model, the figuring technique for the rectifier load identical impedance is checked, and the comparable burden qualities are considered. Right off the bat, exploratory mutilation, which is equivalent to appeared in Fig.2. In addition, import the test information to the product Matlab, and the amplitudes and stage points of the major

waves will be determined through the FFT (quick Fourier change) program. Thus, the basic waves can be drawn by Matlab and appeared in Fig. 8(b). It proposes that the major flood of rectifier input current falls behind the one of rectifier input voltage, which means the rectifier input impedance contains a specific inductance segment. This end is reliable with the one acquired in Section II.



(a) Rectifier input voltage and current waveforms.



(b) Calculated fundamental waves.
Fig. 8. Trial aftereffects

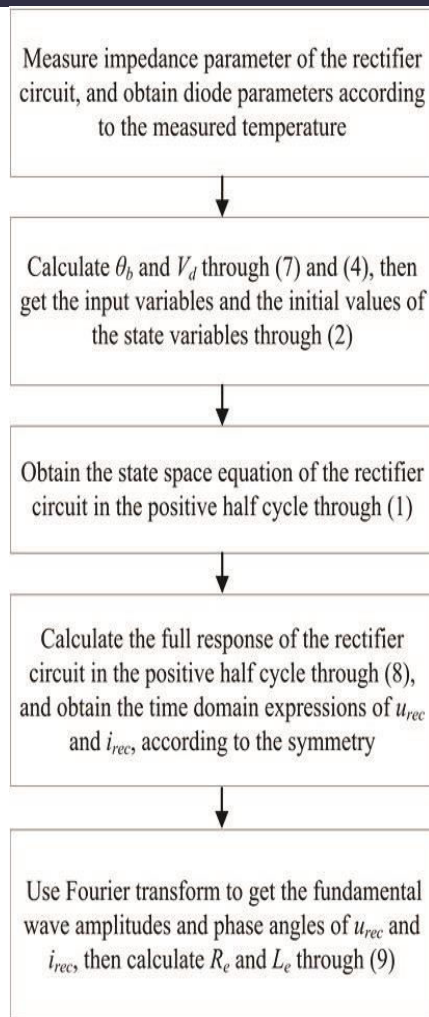


Fig. 9. Stream diagram of the proposed strategy used to ascertain the rectifier comparable burden.

At that point, the rectifier proportionate burden figuring technique is checked on states of various burden protections and rectifier input inductances. In view of the investigation in Section II, the identical opposition and inductance can be determined through the procedure in the stream diagram in Fig.9. Following the means in Fig.9, the equal impedances of the rectifier burden can be determined and given in Tab.1. Likewise, the exploratory ones are appeared in Tab.1, which are acquired from the essential abundancy and stage edge figuring aftereffects of the test waveforms.

Table-1: Its Comparison of Experimental Rectifier Equivalent Loads Based On Different Parameter Values

Prototype Parameter Values		Calculated Equivalent Load		Experimental Equivalent Load	
$R_L (\Omega)$	$L_L (\mu\text{H})$	$R_e (\Omega)$	$L_e (\mu\text{H})$	$R_e (\Omega)$	$L_e (\mu\text{H})$
42.9	83.3	33.1	10.5	33.0	10.2
	113.9	33.8	7.7	33.7	8.2
	49.1	30.4	16.9	32.7	18.2
21.5	83.3	17.1	2.1	17.4	2.5
	113.9	17.3	1.4	17.2	1.7
	49.1	16.6	3.9	17.5	4.6

Tab.1 proposes that the equal opposition and inductance will both decrease when RL decreases. While, the comparable opposition isn't influenced much by L_s , and the equal inductance will increment when L_s decreases. Further estimations demonstrate that on the state of standard parameter esteems, contrast between the determined and test proportionate protections is just 0.1 Ω , and the figuring mistake of the equal inductance is littler than 3%. It implies the proposed strategy has great exactness, when the framework is very much planned and working in the appraised state. Notwithstanding, when L_s is changed to 49.1 μH , the count mistake has expanded to 7%. This is brought about by the estimation of L_s is too little to even consider making the rectifier working in the irregular conduction mode (DCM). Additionally, when RL is changed to 21.5 Ω , the relative mistake rates increment, because of the little estimations of proportionate inductances. In any case, the outright blunders are still little. Along these lines, the determined outcomes are essentially near the test ones, which have demonstrated the viability of the rectifier burden model and the proportionate impedance estimation strategy. In any case, there is a pattern that L_e decreases when RL diminishes. In this way, if RL has a little an incentive around a couple of ohms, L_e will be little. At the point continues as before while the charging current has expanded to

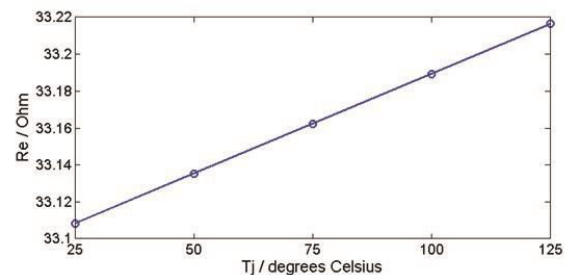
80 An or higher, the identical framework load obstruction will be a couple of ohms. when WCS is utilized for the quick charging of the traveler autos, or the typical charging for the hard core vehicles. The yield intensity of this sort of WCS is typically in excess of 20 kW, even arrives at in excess of 100 kW. Under these conditions, L_e is a lot littler rectifier input inductance L_s , and its impact is unimportant. In any case, the moderate charging for the traveler vehicles (with yield power lower than 10 kW) still hold an extensive extent, so the proposed rectifier comparable burden figuring technique could likewise be valuable for the examination and plan of EV remote charging framework.

In addition, the determined and test estimations of the identical protections are near the ones got by customary technique (34.77 Ω and 17.43 Ω), which receives the coefficient $8/\pi^2$ as the connection between framework load opposition [5,6]. This shows the traditional strategy can be roughly utilized for proportionate opposition count. Be that as it may, it overlooks the identical inductance, just as the impacts of rectifier circuit parameters.

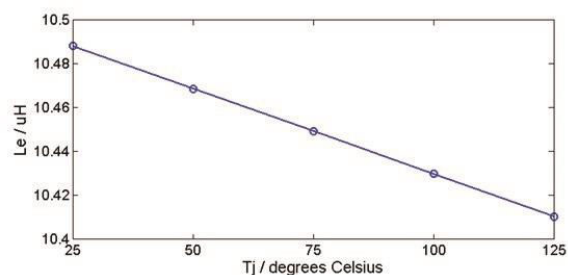
Moreover, impacts of different WCS parameters on the rectifier equal burden examined. At the point when DC source voltage is changed to 200V and different parameters still have standard qualities, determined proportionate burden and 10.6 μH . At the point when the get loop has a horizontal misalignment separation of 10 cm, and different parameters still have standard qualities, the determined proportionate burden is 33.1 Ω and 10.5 μH ; while, the trial one is 32.9 Ω and 10.3 μH . These outcomes propose different WCS parameters, for example, DC source voltage and shared inductance, fundamentally have no impact on the rectifier identical burden. In

this way, the rectifier burden can be demonstrated and dissected decoupling with different pieces of WCS.

Finally, the strength of the proposed rectifier equal burden figuring technique is talked about towards parameter vulnerabilities. The parameter vulnerabilities are for the most part brought about by the estimation mistakes and the stray parameters. Additionally, the diode parameter esteems V_{dio} and R_{dio} will change with the intersection temperature T_j . Since the intersection temperature of the diode can't be estimated straightforwardly, and just can be assessed by the gadget surface temperature, so this will prompt parameter vulnerabilities of the rectifier, as well. The ostensible precision of the LCR meter utilized for estimations is 0.05%. Subsequently, the impact of the estimation mistake will be little, and the effect of T_j is received here to break down the power.



(a) Calculation results of the equivalent resistance R_e .



(b) Calculation results of the equivalent inductance L_e .

Fig. 10. Rectifier equal burden estimation results, when the diode parameter esteems V_{dio} and R_{dio} change with the intersection temperature T_j .

The intersection temperature T_j is generally working conditions. In this way, the rectifier comparable burden computation results are appeared in esteems V_{dio} and R_{dio} change with the intersection temperature T_j . Fig.10 recommends that the difference in the intersection temperature just smally affects the rectifier proportionate burden computation results. Likewise, the past examination demonstrates that the figuring technique can accomplish high precision, on states of various framework load protections, rectifier input inductances, DC voltages, and shared inductances. In this way, the proposed rectifier equal burden computation strategy has great strength, in the instances of WCS parameter varieties. Plus, it ought to be seen charging.

C. Effects of Rectifier Load Equivalent Inductance

Since the customary plan strategies as a rule disregard the proportional inductance of the rectifier load [19-21], we will examine its belongings. Fig.11 demonstrates the reenactment consequences of L_e impacts, which are led by Matlab, as per real parameter estimations of the created EV remote charging model. This reenactment hasn't considered the exchanging misfortunes of influence converters, other stray misfortunes. Thus, the estimations of the mimicked yield forces and efficiencies will be somewhat bigger than the exploratory ones.

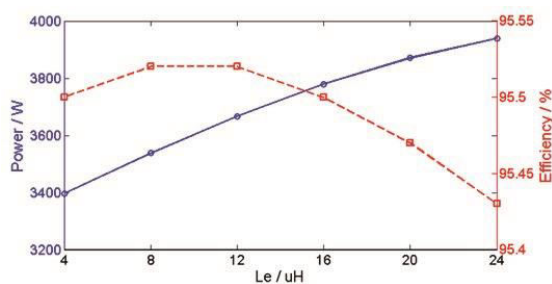
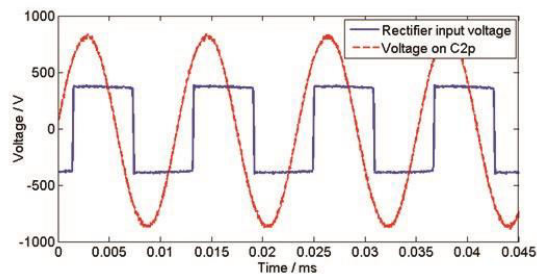


Fig. 11. Reproduction consequences of L_e impacts on yield power and proficiency.

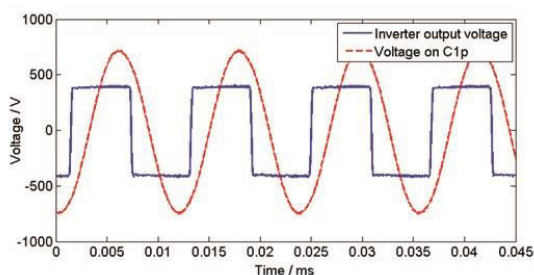
Fig.11 proposes the impact of L_e on proficiency is extremely little. Nonetheless, the yield when L_e differs. Considering the evaluated framework yield control the change range is over 15%, affected by the proportional inductance. Henceforth, L_e will altogether influence the yield control, and the framework yield power will have clear deviation with the appraised one, if the pay systems are planned without thinking about its impact. So as to further demonstrate this end, we have structured another gathering of remuneration capacitors, in light of the traditional $8/\pi^2$ rectifier load computation technique and disregarding L_e . Since the essential and auxiliary side remuneration system structures are decoupled, and L_e just influences the plan brings about the optional side as referenced in Section-III, the optional pay capacitors have been upgraded as pursues: $C_{2s}=22.4$ nF, $C_{2p}=73.3$ nF; while the essential side pay capacitors continue as before. Since the first remuneration capacitors are planned through the technique proposed in Section-III, expect to accomplish the most extreme proficiency and the evaluated yield control simultaneously, which is 3.3 kW for the created EV remote model. The exploratory outcomes have demonstrated that framework proficiency can reach as high as 93.5%, and yield power is 3.33 kW, which is exceptionally near the plan focus of the appraised yield control 3.3 kW, on the state of receiving the first remuneration capacitor esteems. In any case, when overlooking L_e to plan the remuneration capacitors, the trial results demonstrate that the deliberate framework productivity is 93.2%; while the deliberate yield power has expanded to 3.95 kW, which is in excess of 600 W higher than the structure focus of the evaluated yield control. For this situation, the receptive power in WCS will increment, and

carry enormous electric worries to the framework gadgets, even influence the protected activity of WCS. Consequently, these investigations have demonstrated that the comparable inductance of the rectifier load should be considered for framework plan and examination. Likewise, they have demonstrated the viability of the proposed remuneration system structure strategy, which can make WCS accomplish high effectiveness and appraised yield control.

D. Verifications of Load Estimation Methods



(a) Measured voltages used for secondary side load estimation.



(b) Measured voltages used for primary side load estimation.

Fig. 12. Experimental results of the system voltages used for load estimations based on the standard parameter values.

In view of the created EV remote charging model, the proposed auxiliary and essential side burden estimation strategies can be checked. Fig.12 demonstrates the deliberate framework voltages utilized for burden estimations, under the state of standard parameter esteems; where, estimated voltages in Fig. 12(a) are utilized for auxiliary side burden estimation, and the ones in Fig. 12(b) are utilized for essential

side burden estimation. Through these trial results, the positive zero intersection times can be straightforwardly separated from the deliberate information, when the deliberate voltage worth abandons negative to positive. Likewise, the major amplitudes of the deliberate voltages can be determined by the FFT program in Matlab, to get the abundance of the principal voltage move work G_p . So as indicated by the deliberate voltages, the adequacy and stage edge of G_p can be gotten, and the framework load obstruction can be evaluated through the procedure in the stream graph in Fig.13.

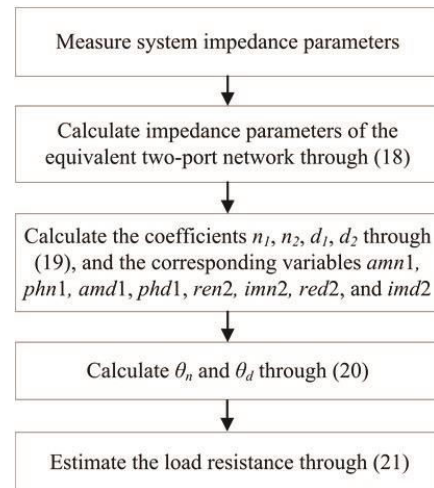


Fig. 13. Stream outline of the proposed burden estimation technique dependent on the deliberate essential side voltages.

Table-II: Load Estimation Results Using Proposed Secondary And Primary Side Load Estimation Methods

Prototype Parameter Values		Secondary Side Load Estimation Method	Primary Side Load Estimation Method
R_L (Ω)	L_s (μ H)	R_{L_Sens} (Ω)	R_{L_Perr} (Ω)
42.9	83.3	41.3	43.5
	113.9	41.5	44.9
	49.1	39.4	44.6
21.5	83.3	21.2	24.4
	113.9	21.3	24.7
	49.1	20.7	24.1

Following the means in Fig.13, the heap estimation results can be gotten and given in Tab.2, on states of various burden protections and rectifier input inductances. Tab.2 recommends that for the auxiliary

side burden estimation strategy, the estimation mistake is 3.7% on the state of standard parameter esteems. This implies the proposed technique has great exactness, when the framework is all around planned and working in the evaluated state. Yet, when L_s is changed to 49.1 μH , the estimation blunder has expanded to 8.2%, because of the DCM working condition of the rectifier. Additionally, when R_L is changed to 21.5 Ω , the most extreme estimation mistake is just 3.7%. The estimation blunders are fundamentally brought about by the estimation deviations of the voltage zero intersection times, and the impacts of the channel capacitor and its stray opposition, which have been disregarded in the underlying worth figuring procedure of the rectifier circuit. In addition, for the essential side burden estimation strategy, Tab.2 proposes its estimation mistake is 1.4% on the state of standard parameter esteems, which means it likewise performs well. In any case, the estimation mistakes clearly increment, on the conditions that R_L is equivalent to 21.5 Ω . This can be clarified by the essential side burden estimation strategy needs the deliberate parameter estimations of WCS, which all have certain estimation deviations. At the point when R_L has changed to 21.5 Ω , the stage edges of the voltage move capacities become greater and closer to 90° , so the estimation deviations will be all the more effectively intensified by the digression work in (21). In addition, the strength of the proposed essential side burden estimation strategy is talked about towards parameter vulnerabilities. The effect of the stray parameter is received to investigate the heartiness here. The real stray parameter in WCS is the inductance of the associating links, which is excluded in the set up framework model. These links are

generally used to associate curls to different parts, or be the lead wires of the inductors. Along these lines, they fundamentally influence estimations of the curls and pay inductances. As per estimations of these links, their stray inductances are littler than or around 1 μH . So as to make its persuasions progressively self-evident, we select this incentive as $\pm 1.5 \mu\text{H}$. Since the stray inductances are too little to even think about being led in analyses, reproductions are received here. Taking the conditions that L_1 has the inductance with $\pm 1.5 \mu\text{H}$ errors for instance, the reenactment results are demonstrated Fig.14. Further computation dependent on Fig.14 shows that the estimation blunder ranges to nearly 6%, when L_1 has the inductance with 1.5 μH mistake. This blunder is clear and the stray inductance ought to be viewed as when evaluating the framework load. In this way, the interfacing links of the curls and the lead wires of the inductors are taken into check, when we quantified the parameter esteems. Since the impacts of the significant stray parameter in WCS are considered, the proposed burden estimation techniques have great strength, on conditions that stray parameters exist.

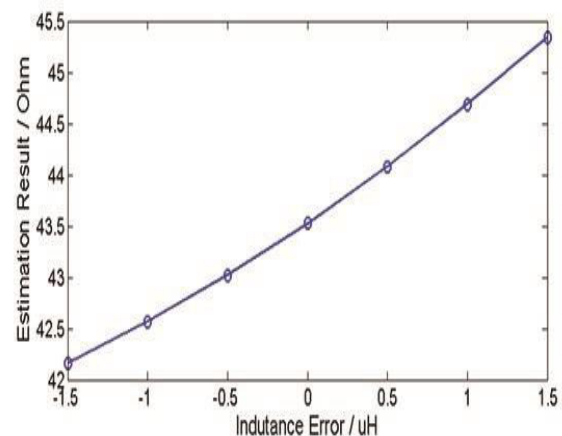


Fig. 14. Mimicked load estimation aftereffects of the proposed essential side strategy, when L_1 has the inductance with $\pm 1.5 \mu\text{H}$ blunders.

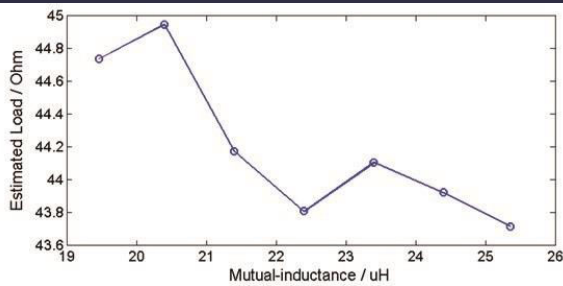


Fig. 15. Reenacted load estimation aftereffects of the proposed essential side technique, when M shifts about 23%.

Moreover, the vigor of the proposed essential side burden estimation technique is demonstrated, when the common inductance M is variable. Through estimation and count, M is 19.5 uH with 15 cm horizontal misalignment. For this situation, M variety is over 23%, when the parallel misalignment separation changes from 0 cm to 15 cm. In view of the genuine parameter esteems, recreated load estimation results are appeared in Fig.15. Further figuring demonstrates that the greatest estimation mistake is littler than 3%, when M differs about 23%. At that point, the analyses demonstrate that when the get curl has a sidelong misalignment separation of 10 cm, and different parameters still have standard qualities, RL_Sesti is 41.7 Ω , and RL_Pesti is 44.7 Ω ; while the estimation blunders are 2.8% and 4.2%, individually. These exploratory mistakes are likewise little. Along these lines, the proposed burden estimation strategies have great heartiness, on states of shared inductance M variety. At last, the heartiness of the proposed essential side burden estimation strategy is examined, when the pay capacitances C1s, C1p, C2s, and C2p have 25% varieties. In light of the genuine parameter esteems, recreated estimation mistake rates are appeared in Fig.16, contrasted and the framework load obstruction 42.9 Ω . In Fig.16, the instances of pay capacitances expanding by 25% are taken as models. Unmistakably the

estimation blunders are nearly in the scope of $\pm 3\%$, when the remuneration capacitances differ 25%. At that point, the exploratory outcomes are given, thinking about the related examination in Section V. C. At the point when the optional side pay capacitances have been changed to 22.4 nF and 73.3 nF, and different WCS parameters still have standard qualities, RL_Sesti will be 40.9 Ω , and RL_Pesti will be 44.2 Ω ; while the estimation mistakes are 4.7% and 3.0%, separately. These exploratory outcomes have demonstrated that the most extreme estimation blunder is under 5%. Along these lines, the proposed burden estimation strategies have great power, on states of remuneration capacitance varieties.

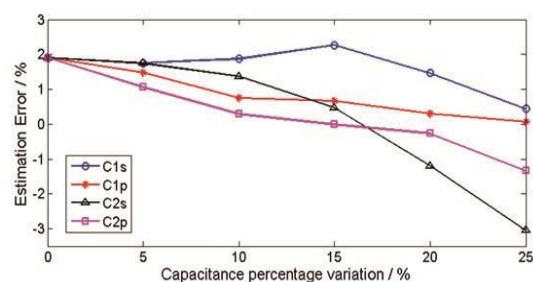


Fig. 16. Reproduced load estimation mistakes of the proposed essential side technique, when the remuneration capacitances differ 25%.

Also, when DC source voltage is changed to 200 V and different parameters still have standard qualities, RL_Sesti is 41.7 Ω , and RL_Pesti is 43.8 Ω ; while the estimation mistakes are 2.8% and 2.1%, individually. In this way, these exploratory outcomes have demonstrated that the proposed burden estimation strategies have great heartiness, on states of DC source voltage variety. To aggregate up, despite the fact that there are a few deviations, the assessed burden protections are essentially near the real estimations of the framework load resistors. This has demonstrated the viability and heartiness of the proposed auxiliary and essential side burden estimation techniques.

Further work might be centered around diminishing the estimation deviation impacts of both the voltages and the WCS parameters, so as to improve the precision of the heap estimation strategies, particularly on conditions that stage points of the voltage move capacities are near 90° .

VI. CONCLUSION

This paper exhibits an orderly investigation of the rectifier burden utilized for EV remote charging framework. The rectifier burden model has been set up to figure its identical information impedance, which contains both obstruction and inductance segments, and can be freely determined through the parameters of the rectifier circuit. In light of the rectifier load investigation, a pay system structure strategy is proposed to accomplish the decoupling plan of the essential and auxiliary side remuneration capacitors. Moreover, an optional side burden estimation strategy and an essential side burden estimation technique are advanced, considering the impact of the rectifier load. They embrace just estimated voltages to dodge the deviations presented by various stage delays between estimated voltage and current. At long last, the set up model, the proposed rectifier load figuring technique, remuneration system plan strategy, auxiliary and essential side burden estimation strategies have been confirmed, in view of the created EV remote charging model. The exploratory outcomes have demonstrated the accompanying ends: the equal information impedance of rectifier burden is primarily influenced by framework load opposition and rectifier input inductance; rectifier load comparable inductance will affect framework exhibitions, and ought to be considered for pay system structure; the proposed burden estimation strategies of great precision, yet at the same time should be improved in further research; the

proposed rectifier load computation strategy and framework load estimation techniques all have great strength, states of WCS parameter varieties. In spite of the fact that the works in this paper are directed dependent on the particular framework, they can be stretched out to more applications, for example, remote accusing frameworks of other rectifier or remuneration organize topologies, and so on. They will be useful for framework structure and control to make EV remote charging frameworks accomplish stable activity & superior.

REFERENCES

- 1) S.Q.Li, and C.C.Mi, "Wireless power transfer for electric vehicle applications," *IEEE J. Emerg. Sel. Topics Power Electron.*, vol.3, no.1, pp.4-17, Mar 2015.
- 2) Y.D.Ko, and Y.J.Jang, "The optimal system design of the online electric vehicle utilizing wireless power transmission technology," *IEEE Trans Intell Transp. Syst.* vol.14, no.3, p. 1255-1265, Sep. 2013.
- 3) W.X.Zhong, and S.Y.R.Hui, "Maximum energy efficiency tracking for wireless power transfer systems," *IEEE Tran Power Electron.*, vol.30, no.7, pp.4025-4034, July 2015.
- 4) D.Ahn, S.Kim, J.Moon, and I.K.Cho, "Wireless power transfer with automatic feedback control of load resistance transformation," *IEEE Tran Power Electron.* vol.31, no.11, pp.7876-7886, Nov. 2016.
- 5) M.P.Theodoridis, "Effective capacitive power transfer," *IEEE Trans Power Electron* vol.27, no.12, pp.4906-4913, Dec. 2012.
- 6) D.Thenathayalan, and J.H.Park, "Wide-air-gap transformer model for the design-oriented analysis of contactless power converters," *IEEE Tran Ind Electron.*, vol.62, no.10, pp.6345-6359, Oct. 2015.

- 7) M.Fu,Z.Tang,M.Liu,C.Ma,andX.Zhu,“Full-bridge rectifier input reactance compensation in megahertz wireless power transfer systems,” in Proc. 2015 WoW, 2015, pp. 1-5.
- 8) Berger,M.Agostinelli,S.VestiJ.A.Oliver,J.A.Cobos,andM.Huemer“A wireless charging system applying phase-shift and amplitude control to maximize efficiency and extractable power,”IEEETrans.Power Electron.,vol.30,no.11,pp.6338-6348,Nov. 2015.
- 9) K.Colak,E.Asa,M.Bojarski,D.Czarkowski and O.C.Onar,“A novel phase-shift control of semibridgeless active rectifier for wireless power transfer,”IEEETrans. PowerElectron.vol30,no.11,pp.6288-297, Nov.2015.
- 10) Y.Akihara,T.Hirose,S.Masuda,N.Kuroki,M.NumaandM.Hashimoto,Analytical study of rectifier circuit for wireless power transfer systems,” in Proc. ISAP, 2016, pp. 338-339.